Homology-Based Prediction of Potential Protein–Protein Interactions between Human Erythrocytes and *Plasmodium falciparum*

Gayatri Ramakrishnan[1,2], Narayanaswamy Srinivasan[2], Ponnan Padmapriya[3] and Vasant Natarajan[3]

[1]Indian Institute of Science Mathematics Initiative, Indian Institute of Science, Bangalore, India. [2]Molecular Biophysics Unit, Indian Institute of Science, Bangalore, India. [3]Department of Physics, Indian Institute of Science, Bangalore, India.

ABSTRACT: *Plasmodium falciparum*, a causative agent of malaria, is a well-characterized obligate intracellular parasite known for its ability to remodel host cells, particularly erythrocytes, to successfully persist in the host environment. However, the current levels of understanding from the laboratory experiments on the host–parasite interactions and the strategies pursued by the parasite to remodel host erythrocytes are modest. Several computational means developed in the recent past to predict host–parasite/pathogen interactions have generated testable hypotheses on feasible protein–protein interactions. We demonstrate the utility of protein structure-based protocol in the recognition of potential interacting proteins across *P. falciparum* and host erythrocytes. In concert with the information on the expression and subcellular localization of host and parasite proteins, we have identified 208 biologically feasible interactions potentially brought about by 59 *P. falciparum* and 30 host erythrocyte proteins. For selected cases, we have evaluated the physicochemical viability of the predicted interactions in terms of surface complementarity, electrostatic complementarity, and interaction energies at protein interface regions. Such careful inspection of molecular and mechanistic details generates high confidence on the predicted host–parasite protein–protein interactions. The predicted host–parasite interactions generate many experimentally testable hypotheses that can contribute to the understanding of possible mechanisms undertaken by the parasite in host erythrocyte remodeling. Thus, the key protein players recognized in *P. falciparum* can be explored for their usefulness as targets for chemotherapeutic intervention.

KEYWORDS: homology-based approaches, host–parasite interactions, protein–protein interactions, *Plasmodium falciparum*

CITATION: Ramakrishnan et al. Homology-Based Prediction of Potential Protein–Protein Interactions between Human Erythrocytes and Plasmodium falciparum. *Bioinformatics and Biology Insights* 2015:9 195–206 doi: 10.4137/BBI.S31880.

TYPE: Original Research

RECEIVED: July 16, 2015. **RESUBMITTED:** November 08, 2015. **ACCEPTED FOR PUBLICATION:** November 14, 2015.

ACADEMIC EDITOR: Thomas Dandekar, Associate Editor

PEER REVIEW: Seven peer reviewers contributed to the peer review report. Reviewers' reports totaled 1908 words, excluding any confidential comments to the academic editor.

FUNDING: This research was supported by the Mathematical Biology Program sponsored by the Department of Science and Technology and the Department of Biotechnology, Government of India, as well as by Microsoft Corporation. This work was also supported by the University Grant Commission (UGC), Government of India, under the scheme D.S. Kothari postdoctoral fellowship (Ref No: F.4-2/2006(BSR)/13-610/2012(BSR)). PP is a D.S. Kothari postdoctoral fellow. NS is a J.C. Bose National Fellow. The authors confirm that the funder had no influence over the study design, content of the article, or selection of this journal.

COMPETING INTERESTS: Authors disclose no potential conflicts of interest.

CORRESPONDENCE: ns@mbu.iisc.ernet.in

Introduction

Malaria, a potentially lethal mosquito-borne disease, has existed as a public health burden for many decades, currently placing 1.2 billion of the world's population at high risk.[1] This disease is caused by parasites belonging to *Plasmodium* genus. Of the five species of parasites known to cause malaria, *Plasmodium falciparum*, *Plasmodium vivax*, *Plasmodium malariae*, and *Plasmodium ovale* are pathogenic to human, of which *P. falciparum* is the most prevalent. *P. falciparum* is essentially an obligate intracellular parasite with a complex life cycle, exhibiting varied morphological stages in different tissue types in two different hosts: humans and female mosquitoes of the genus *Anopheles*.[2] The remarkable ability of the parasite to adapt to varied challenges posed by the hosts, in terms of heterogeneous environmental conditions and immunological responses, has facilitated successful pathogenesis and persistence of the parasite over the course of coevolution with its hosts.

In addition to the adaptive changes brought about by the vast reorganization of cellular processes, the parasite has also the capability to remodel host cells, particularly erythrocytes, to suit its niche during infection. During a blood meal of a mosquito vector, motile infective form of parasite known as sporozoites are injected into the blood stream, which then travel to liver where they undergo rapid multiplication and differentiation to generate large number of merozoites. The blood stages of infection begin once these merozoites released from liver cells invade the erythrocytes. Throughout the intraerythrocytic stages of the parasite's life cycle, including ring, trophozoite, and schizont, the parasite establishes intricate mechanisms to remodel erythrocytes for its growth and survival.[3] Exploitative mechanisms achieved by the parasite include the acquisition of nutrients from the cytosol of red blood cells (RBCs) and from extracellular environ, mediation of cellular adhesion of infected RBCs to avoid splenic

clearance, evading host immune response by associating antigenically variant proteins with erythrocyte surface, and the establishment of protein-trafficking machinery. Much of these mechanisms can be attributed to the parasite proteins targeted to RBC membrane.[4,5] The intricateness in the massive remodeling of host RBCs induced by the parasite and the unusual plasticity of the parasite's metabolism through the various stages of its life cycle has been well studied.[3–6] Moreover, the characterization of *P. falciparum*-infected and -uninfected RBCs with the help of optical tweezers, pursued previously by one of our groups, has provided a novel insight into the biomechanical properties of infected and uninfected cells.[7] An interesting phenomenon observed is termed as *bystander effect*, which is the effect of infected RBCs on the physical properties of uninfected RBCs.[7] This observation concurs with a similar established finding on exosome-like vesicles, proposed to participate in intercellular communication between infected RBCs.[8] Despite the tremendous efforts in providing useful insights on RBC–parasite interactions, much of our understanding on molecular basis of host–parasite interactions is limited, essentially based on inferences obtained from experimental evidences.

Over the past several years, substantial efforts have been made toward the development of computational framework to predict protein–protein interactions with the help of evolutionary information[9,10] that are primarily based on experimentally known interactions documented in various databases. However, interactions identified based on homology alone need rigorous evaluation in order to filter interactions in biological context. Functionally relevant interactions can be systematically identified by the use of molecular details of three-dimensional (3-D) structures of protein–protein complexes. By virtue of similarity to the structure of a protein complex, it is possible to determine and assess putative interacting residues in the homologous protein pair based on conservation. The credibility of the predicted interactions can then be enhanced by integrating additional information such as gene expression and subcellular localization in order to assess their ability to bind physically in the pathological context. The significance of such structure-influenced transfer of interactions between organisms has been realized and has formed the basis of several frameworks.[11–13] On similar grounds, computational efforts to predict protein–protein interactions across human and pathogen(s) of interest have been successfully achieved by many groups[14,15] as well as by one of our groups earlier.[16–19]

The availability of completely sequenced genome of human and *P. falciparum*[20] and the rich catalog of experimentally determined interaction datasets has aided thorough computational investigations on probable protein–protein interactions within the parasite[21] as well as across human and the parasite.[22] Albeit elaborate, the proposed approach on predicting host–parasite interactions lacks stringent evaluation of the predicted protein partners in endogenous context. Integrating subcellular localization data of both host and parasite proteins forms a critical filtering step as a pair of proteins predicted to interact may not be biologically feasible if they are localized in different compartments of the cell. In our previous study,[16] we presented a data integration approach in order to detect protein–protein interactions across human host and *P. falciparum*, where information from experimentally identified protein–protein interaction datasets coupled with expression and subcellular localization data aided the identification of feasible host–parasite interactions. Much recently, a data intensive machine-learning approach was also employed[23] to predict protein interactions across human and *P. falciparum*. However, the inaccuracies in genome-scale high-throughput protein–protein interaction datasets that are used by these approaches raise concern on false positives in the predictions. In a recently published study by one of our groups,[19] an attempt was made to circumvent the dependence on high-throughput interaction data by considering an initial refined dataset of 3-D structures of protein complexes alone, to predict potential interactions across human host and *Mycobacterium tuberculosis* H37Rv. We demonstrate the utility of such a structural similarity-based protocol to predict biologically feasible protein–protein interactions across *P. falciparum* and host erythrocytes. The likelihood of these interactions is suggested by the information on expression profiles and subcellular localization of proteins involved and, most importantly, the 3-D structural compatibility to interact. For specific cases, we have pursued rigorous evaluation in terms of surface complementarity, electrostatic complementarity, and interaction energy at the interface regions to support the credibility of the predictions made.

Methodology

Datasets considered. Protein sequences of 5542 gene products of *P. falciparum* 3D7 were obtained from PlasmoDB (Version 12),[24] while for human red blood cell proteins, a recently updated and improved dataset of RBC proteome[25] was consulted, which reports a nonredundant list of 1989 gene products. We mapped this list to UniProt database[26] to obtain sequence information and annotations for RBC proteins, followed by the use of filters to exclude incomplete protein sequence entries (fragments), thus obtaining a final set of 1672 RBC proteins.

To pursue structure-influenced recognition of protein interactions, two datasets were used: (i) a cumulative dataset of structures of transient protein–protein complexes published earlier[27–29] and (ii) a dataset of domain-centric protein–protein interactions from Protein Family Interactions (iPfam) database.[30] iPfam database provides a comprehensive resource of domain–domain interactions that are formulated using combined information from the structures of protein complexes in Protein Data Bank[31] and their constituent sequence domains acquired from Protein Family (Pfam) database.[32] Since the current definitions are primarily based on the calculations performed on asymmetric unit of protein complexes, we have restricted our dataset specifically to those interaction

definitions where the crystal asymmetric unit of a protein complex corresponds to a whole biological assembly. For the current analysis, we have considered heterodomain interactions from iPfam, ie, interactions between different protein domain families.

Generation of initial host–parasite interaction dataset. The identification of host and parasite proteins homologous to a known pair of interacting proteins forms the primary step in the recognition of host–parasite protein–protein interactions.

In order to determine homologs of structures of transient protein–protein complexes, we used family specific structural identifiers catalogued in the database of Structural Classification of Proteins (extended version SCOPe 2.04).[33] SCOP, an extensive database of manually curated protein structural relationships, hierarchically classifies protein domains into class–fold–superfamily–family based on structural and evolutionary relationships. A family specific identifier or SCOP code for a structural domain holds the information pertaining to its corresponding classification. Since evolutionarily related proteins tend to exhibit interactions in a similar manner, the family specific SCOP identifiers retrieved for transient protein–protein complexes were mapped to those identified in RBC and parasite proteins. The identification of SCOP domains in RBC and parasite proteins involved a search against a database of profile hidden Markov models[34] (HMMs) representing domains in proteins of known structure, at an *E*-value threshold of 0.0001. The profile HMMs of protein domains were retrieved from SUPERFAMILY database.[35] Similarly, protein sequence searches were also pursued against a database of HMMs representing Pfam domain families. The reliability of the Pfam domain assignments made was assessed using domain family specific gathering thresholds assigned by curators,[36] which roughly correspond to an *E*-value cutoff of 0.01. The interactions between a pair of Pfam domain families suggested in iPfam database and the interactions between a pair of family specific SCOP identifiers obtained from the dataset of transient protein–protein complexes were thus used to predict putative interactions across domain families of RBC and parasite proteins. Appropriate filters were used to achieve biologically relevant protein–protein interactions across host RBC and the parasite, as discussed further.

Filter 1: Refining the template dataset. iPfam attributes the terms intrachain and/or interchain interactions to domains in a protein complex on the basis of the nature of polypeptide(s) and their proximity in the 3-D structures. We excluded the intrachain heterodomain interactions retrieved from iPfam, which were mapped to a single host RBC or a single parasite protein, as such interactions are less likely to occur across species. We had observed that homologs of co-occurring heterodomains in a multidomain protein rarely correspond to two different interacting proteins.[37] Considering this established observation, the exclusion of intrachain heterodomain interactions from the template dataset minimized the occurrence of false-positive predictions. Protein–protein complexes that constituted synthetic constructs were also eliminated. All the protein complexes and the putative RBC–parasite protein–protein interactions deduced were manually curated to ensure their biological relevance.

Filter 2: Pruning intrahost interactions. Similar to the pruning steps in our previously published study,[19] we did not consider intrahost and intrapathogen interactions in our subsequent analyses. These interactions usually correspond to ubiquitous interactions that are conserved within most organisms. We also eliminated those RBC–parasite interactions where the RBC proteins are also capable of exhibiting intrahost interactions. In other words, when the interfacial region of an intrahost protein–protein interaction is comparable to that of a host–parasite interaction, by virtue of similarity of host and parasite proteins to a single template protein complex, the predicted RBC–parasite interactions are not considered. This step ensured the recognition of targetable host–parasite protein–protein complexes. iPfam attributes the terms intrachain and/or interchain interactions to domains in a protein complex on the basis of the nature of polypeptide(s) and their proximity in the 3-D structures. We excluded intrachain heterodomain interactions retrieved from iPfam, which were mapped to a single host RBC protein.

Filter 3: Integrating additional information to extract biologically feasible interactions. Expression profile of parasite proteins for merozoite, ring, trophozoite, and schizont stages was extracted from PlasmoDB and mainly from three studies published earlier.[38–40] Information on subcellular localization of parasite proteins was obtained from diverse sources. The parasite proteins that have been reported to constitute a host-targeting signal, ie, HT motif or PEXEL motif,[41,42] and the exported proteins reportedly lacking PEXEL/HT motif (PNEPs)[43] were picked up. This criterion is of primary importance in recognizing feasible protein–protein interactions across *P. falciparum* and erythrocyte as the parasite resides within a protective encasing termed as parasitophorous vacuole during its intraerythrocytic development. Furthermore, to recognize putative interactions brought about by membrane proteins of the vacuole, we included parasite proteins that are established as parasitophorous vacuole membrane proteins.[44] We also included parasite proteins associated with a specialized secretory compartment, Maurer's cleft.[45] Only those proteins of Maurer's cleft were considered that are either membranous or comprise an export signal. Merozoite surface proteins involved in host RBC invasion were also included.[46] The parasite proteins localized to the apicoplast and other cellular organelles were excluded since the associated proteins may not participate in a physical interaction with RBC proteins.

The subcellular localization data for RBC proteins (membrane, cytoskeleton, or cytosolic) were obtained from UniProt. This information becomes notably crucial in the RBC-*P. falciparum* system, where the parasite proteins specifically target enucleated or mature RBCs that lack nucleus and most of the cellular organelles. The RBC proteins localized to nuclear fractions and other cellular organelles were excluded

as such proteins could be remnants of degraded proteins of ancestral reticulocytes.[25]

Given the set of 5542 parasite proteins and 1672 erythrocyte proteins, the number of possible interactions across the host erythrocyte and the parasite proteins is tremendously large. The use of appropriate filters at various levels, as discussed above, reduces false-positive predictions, thereby resulting in the recognition of probable host–parasite interactions in the endogenous context. Table 1 outlines the number of protein–protein interactions in the initial stages and the reduction in the number of false positives upon the inclusion of filters.

A schematic representation of the protocol followed is shown in Figure 1.

Results and Discussion

Probable host–parasite interactions and their influence on biological processes. The structure-influenced predictions in concert with a series of filters facilitated recognition of 208 physicochemically viable interactions accomplished by 59 *P. falciparum* and 30 host erythrocyte proteins. The distribution of 59 *P. falciparum* proteins across the intraerythrocytic stages is illustrated with the help of a Venn diagram in Figure 2. As depicted in the Venn diagram, the parasite proteins potentially involved in RBC–parasite interaction are distributed throughout the four stages, with highest (13) specific to the ring stage.

The potential influence on pathways and processes in RBC and the parasite were investigated based on the biologically feasible protein–protein interactions predicted across RBC and parasite proteomes. Functional annotations of the parasite proteins were obtained from PlasmoDB and the Malaria Metabolic Pathways database[47] and those of RBC proteins were retrieved from UniProt database. The putatively interacting protein pairs across the parasite proteins and the host RBC could be segregated into 11 and 10 functional categories, respectively, on the basis of the nature of their biological processes. Figure 2 illustrates the intraerythrocytic stage-specific distribution of 59 *P. falciparum* proteins across its 11 functional categories (including conserved protein and cysteine repeat). Each bar represents the number of parasite proteins associated with a functional category, color coded based on stage-specific expression of its constituent proteins. The total number of host RBC proteins predicted to interact with the parasite proteins under each category is denoted by numbers in brackets. Also indicated in Figure 2 is the information on subcellular localization of parasite proteins pertaining to a functional category represented in the form of single letter tags. Evidently, a significant proportion of host–parasite interactions are potentially mediated by exported proteins followed by merozoite surface proteins of the parasite, as illustrated in the figure. This is in corroboration with well-studied observations on parasite proteins that induce host erythrocyte remodelling.[4]

In addition to the host–parasite interactions potentially brought about by parasitic proteins belonging to nine functional categories (rosette formation, kinase, RBC invasion, protease, protein traffic, immune evasion, adhesion, chaperone, and merozoite egress), we could identify two parasite conserved proteins of unknown function (PF3D7_0911300 and PF3D7_1463900), one of which is a cysteine repeat modular protein capable of influencing varied processes in host RBC. This finding is schematically detailed in Figure 3, which exemplifies the participation and the influence of the parasitic processes and pathways on the host cellular roles. The central sliced doughnut in the figure enumerates the parasite proteins under each functional category, and the number of host–parasite interactions influencing host cellular processes is represented as bars corresponding to each slice of the doughnut. Majority of the host–parasite interactions, as depicted in the figure, are mediated by parasite proteins participating in erythrocyte rosetting. Indeed, these proteins belong to the hypervariable *P. falciparum* erythrocyte membrane protein 1 family, encoded by *var* genes, which are known to mediate cytoadhesion of infected erythrocytes.[48] The predominant influence on RBC proteins involved in cell adhesion and immune response, as shown in Figure 3, is in support of the established observation. Notably, RBC proteins involved in signal transduction (27 interactions), followed by RBC chaperones (17 interactions), are also potentially acted upon by the parasites. This observation is in conjunction with the exploitative mechanisms acquired by the parasite to maximally benefit from the host, which include the activation of various cellular signaling pathways and recruitment of host chaperones in order to mediate cytoadherence and establish protein-trafficking machinery for successful persistence in the host.[49,50]

Thus, our structure-based approach has the potential to complement established experimental findings and could provide suitable grounds to warrant an experimental follow-up. Table 2 summarizes the selected examples of interest. The complete list of putative RBC–parasite interactions is provided in Supplementary Table 1. Comparison with previously published

Table 1. Recognition of functionally relevant interactions upon inclusion of appropriate filters, as discussed in the Methodology section.

	NUMBER OF PARASITE PROTEINS EXPRESSED DURING INTRA-ERYTHROCYTIC STAGES	NUMBER OF ERYTHROCYTE PROTEINS	NUMBER OF POTENTIAL PROTEIN–PROTEIN INTERACTIONS
Filter 1	1567	1296	14,965
Filter 2	770	646	6775
Filter 3	59	30	208

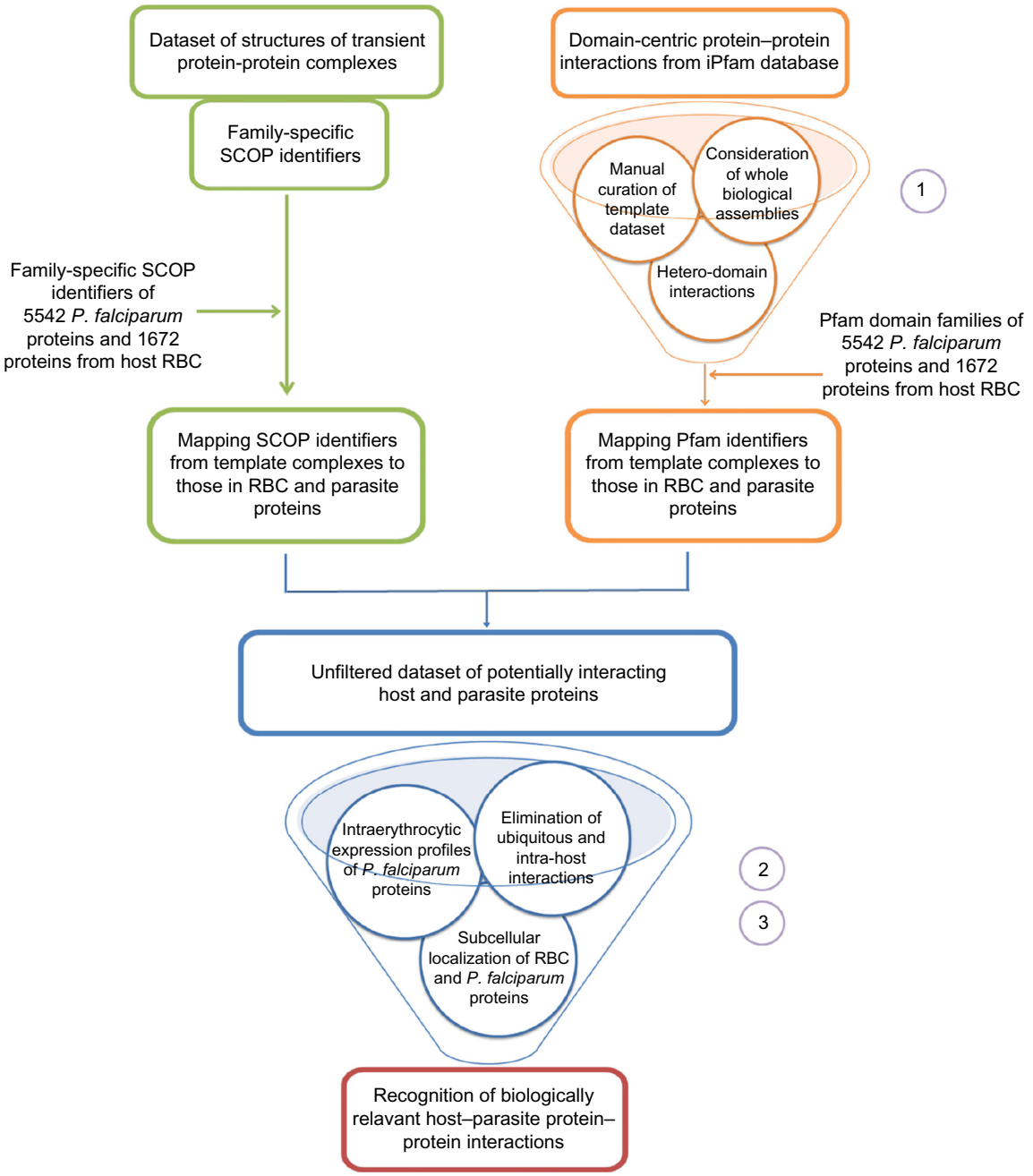

Figure 1. Workflow. A schematic diagram of the steps taken to generate host–parasite protein–protein interaction dataset is shown. The steps start with the consideration of two datasets of transient protein–protein complexes, followed by the identification of their homologs in host and the parasite proteome. The encircled numbers correspond to equivalent subsections on filters in the Methodology section, which facilitated the recognition of biologically relevant host–parasite protein–protein interactions.

computational studies on the identification of host–parasite protein–protein interactions[16,23] yielded a set of five interactions mediated by three parasite proteins and four host proteins, which concurred with our predictions made. Interestingly, we also recognized three host–parasite interactions that concurred with experimental observations. These include interactions mediated by three erythrocyte-binding antigen proteins of the parasite, which bind to erythrocytes in a sialic acid-dependent manner.[51] The host–parasite interactions in concordance with earlier studies are highlighted in Supplementary Table 1.

Investigations on selected cases at the molecular level are discussed further.

Case study 1: Establishment of host–parasite protein-trafficking machinery. The parasite protein, SAR1 (PF3D7_0416800), is a small GTP-binding protein of 192 amino acid residues, which is involved in the crucial step of budding reaction in vesicle-mediated secretory pathway. Based on our protocol, we recognized one protein from host RBC as plausible interacting partner of SAR1. The predicted interaction between SAR1 and the host ADP-ribosylation

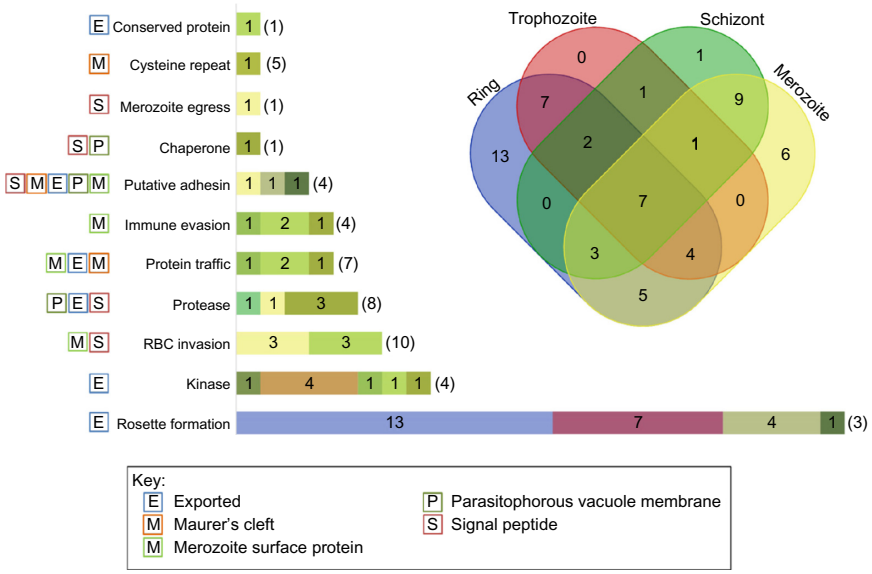

Figure 2. A schematic summary of RBC–parasite interactions. The stage-specific protein expression profiles of the parasite proteins are illustrated in the Venn diagram, while the bar graph depicts the number of parasite proteins under each functional category predicted to interact with host RBC proteins (denoted in brackets). The color codes in each bar are in correspondence with the color of stage-specific expression subsets shown in the Venn diagram. The single letter tags for all the functional categories of the parasite provide information on subcellular localization. The Venn diagram was created using an online tool (http://bioinformatics.psb.ugent.be/webtools/Venn/).

Figure 3. Influence of host–parasite interactions on biological processes and pathways. The central sliced doughnut represents 59 *P. falciparum* proteins, which are classified into 11 categories (slices) on the basis of biological pathways and processes. The bars environing the central doughnut correspond to the number of host–parasite interactions, associated with parasite proteins (each slice), that influence each of the host cellular processes. For textual clarity, the length of the bars has been scaled with respect to each slice.

Table 2. Details of few examples of proteins in *P. falciparum* predicted to interact with host RBC proteins.

P. FALCIPARUM GENE ID	BIOLOGICAL PROCESS/PROTEIN PRODUCT	EVIDENCE OF STAGE-SPECIFIC EXPRESSION OF THE PARASITE PROTEIN				SUBCELLULAR LOCALIZATION	INTERACTING PARTNER IN HOST RBC (UniProt ID)	SUBCELLULAR LOCALIZATION	BIOLOGICAL PROCESS
		RING	TROPHOZOITE	SCHIZONT	MEROZOITE				
PF3D7_0100100	Rosette formation	Y	N	N	N	Exported	P10747	Cell membrane	Immune response
PF3D7_0502400	Putative adhesin	Y	N	N	Y	Parasitophorous vacuole membrane, Merozoite surface	P07996	Cell surface	Cell adhesion
PF3D7_0416800	Protein traffic	Y	Y	Y	Y	Exported (vesicles)	Q9NZ52	Cell membrane	Transport
PF3D7_1408100	Protease	Y	Y	Y	Y	Parasitophorous vacuole membrane	P02549	Cytoskeleton	Cell shape
PF3D7_1463900	Conserved protein	N	N	Y	Y	Exported (HTmotif)	O15554	Cell membrane	Ion channel

factor-binding protein GGA3 (Q9NZ52) is further investigated. The proteins SAR1 and GGA3 were recognized to be evolutionarily related to a protein complex (GTP-bound ADP-ribosylation factor, ARF-GTP, and GAT domain of ADP-ribosylation factor-binding protein GGA1) that demonstrates molecular basis of membrane recruitment of adaptor proteins such as GGA by ARF-GTP. This protein complex elucidated for a mammalian system plays a key role in vesicular transport by docking the adaptor protein GGA1 to membrane for increased efficiency in recognition of cargo receptors.[52] The GAT domain of GGA1 reportedly undergoes conformational change to interact with ARF-GTP. The helix–loop–helix structure, acquired by the disordered N-terminal region of GAT domain, interacts with an interswitch region formed by two antiparallel β strands of ARF-GTP. This ARF-binding disordered region is conserved across the GAT domains of human GGAs, as demonstrated earlier.[52]

To assess the molecular and mechanistic details of the host–parasite interaction mediated by the protein pair GGA3–SAR1, the disordered region (166–210) of the 723 residue protein GGA3 was modeled using MODELLER v.9.14[53] with the help of template helix–loop–helix structure of GAT domain of GGA1, while reliable structural model for SAR1 (region: 22–191, model coverage: 89%) was obtained from ModBase, which is a large-scale comprehensive database of comparative protein structure models.[54] The models built were assessed for local structural matches with respect to the template protein complex using TM-align.[55] The program assigns TM-score for a structurally aligned protein pair, which typically acquires a value in (0, 1]. A TM-score of ≥0.50 corresponds to convincing structural similarity, and a TM-score of <0.30 depicts random structural matches.[56] Table 3 provides an account of sequence and structural assessment of the host–parasite protein pair under investigation. As depicted in Table 3, a TM-score >0.9 could be achieved for both host and parasite protein structural models. Thus, GGA3–SAR1 protein–protein interaction was modeled using the template protein complex and a subsequent energy-minimization step was pursued using GROMACS (Version 4.5.5)[57] to achieve a stable form of the modeled complex. The putative host–parasite protein complex was then assessed for the conservation of interfacial residues. Figure 4 highlights the key conserved residues in the predicted GGA3–SAR1 complex. The predominant participation of hydrophobic residues at the interface, as shown in Figure 4, is similar to the hydrophobic interactions observed at the interface of the template protein complex,[52] thus, suggesting usefulness of the predictions made. Additional comparative assessments in terms of shape complementarity and interaction energies at the interfacial region of GGA3–SAR1 protein complex were also pursued to evaluate our predictions further. We employed a shape correlation statistic S_c, availed through CCP4 suite of programs,[58] to quantify geometrical packing of the interface of the predicted protein complex. S_c acquires a value from 0 to 1, where an S_c measure of 1 suggests

Table 3. Details on sequence and structural assessment of the predicted host–parasite protein pair GGA3–SAR1.

PROTEINS IN TEMPLATE COMPLEX (PDB CODE: CHAIN ID)	LENGTH OF THE PROTEIN/ DOMAIN	HOMOLOGOUS PROTEIN		LENGTH OF THE PROTEIN/ DOMAIN	SEQUENCE IDENTITY BETWEEN TEMPLATE AND THE PROTEIN OF INTEREST	TM-SCORE BASED ON STRUCTURAL ALIGNMENT TOOL TM-ALIGN	NUMBER OF TOPOLOGICALLY EQUIVALENT RESIDUES
ARF-GTP 1J2J:A	166	*P. falciparum*	SAR1	192	35%	0.91	159
GAT domain of GGA1 1J2J:B	45	Human RBC	GGA3	45 (GAT domain: 166–210)	64.4%	0.99	41

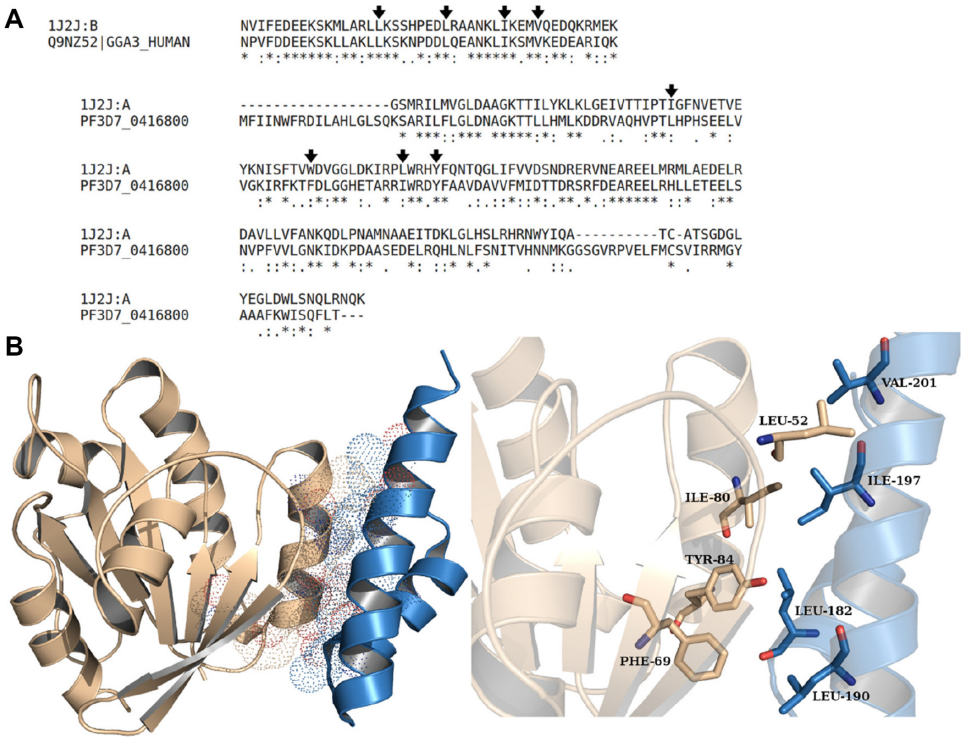

Figure 4. Assessment of putative host–parasite protein pair GGA3–SAR1. (**A**) Sequence alignment of GAT domains of GGA3 and GGA1 (1J2J:B) and of SAR1 and ARF-GTP (1J2J:A) is described. The conserved interfacial residues are indicated with black arrows. (**B**) Probable binding pose of the predicted host–parasite interaction is shown in the illustration on the left panel, while the figure in the right panel delineates the residues participating in the GGA3–SAR1 interaction. The structures in Figure 4, 5, and 7 are generated using PyMOL (http://www.pymol.org/).[71]

perfectly complementing interacting surfaces, while an S_c value approximating to zero implies an interacting surface of uncorrelated topology. The shape correlation statistic for the template protein complex was determined to be 0.7, while the S_c measure recognized for the GGA3–SAR1 protein complex was 0.57, indicating comparable geometrical packing at the interfacial regions of the template and the modeled complex. Assessment of interaction energy for the host–parasite protein pair using FoldX,[59] an empirical effective energy function, yielded a comparable binding energy value of –12.14 kcal/mol against an interaction energy value of –16.86 kcal/mol obtained for the template complex crystal structure.

The significance of SAR1 in establishing protein-trafficking machinery in infected erythrocytes has been well demonstrated earlier. It has been postulated that SAR1 gets translocated to erythrocyte cytosol through a specialized secretory organelle, where it participates in trafficking proteins to erythrocyte membrane.[60,61] These established observations are in successful accordance with the proposed GGA3–SAR1 protein–protein interaction, thus, implying functional relevance of probable host RBC-assisted protein-trafficking machinery brought about by the parasite.

Case study 2: Strategies acquired by the parasite to proliferate in the host environment. Calcium, a well-studied intracellular messenger in eukaryotes, is known to play a significant role in the regulation of diverse cellular processes and interactions. Several calcium ion-mediated processes are facilitated by the calcium-binding protein calmodulin. One such process is the regulation of cell membrane potential by calcium-activated potassium channels. The proper functioning of potassium channels aids in the regulation of intracellular osmolarity, membrane potential, and electrochemical

gradient, thus, forming an integral part of cellular viability.[62] The chemomechanical gating mechanism for such potassium channels has been elucidated at the molecular level, earlier,[63] where calcium-bound calmodulin reportedly binds to the channel and triggers its opening. The crystal structure of calmodulin–potassium ion channel complex elucidates the heterotetrameric association of calmodulin and calmodulin-binding domain of ion channel, that is, dimer of heterodimer. The oligomeric state of calmodulin and calmodulin-binding domain is a dimer in the absence of calcium ions, while the binding of calcium ions to calmodulin triggers the formation of an elongated heterotetrameric complex (Fig. 5), resulting in a rotary movement of the two calmodulin-binding domains, thus, serving as gates to drive open the channel.[63] Based on the structure-influenced approach, we identified probable interaction between host calcium-activated potassium channel protein 4, KCNN4 (UniProt ID: O15554), and conserved parasitic protein of unknown function, PF3D7_1463900.

PF3D7_1463900, a conserved parasitic protein of unknown function of 1071 amino acid residues, was identified to constitute an EF-hand domain region (calcium-binding protein) at its C-terminal end (896–1054). A reliable structural model, using MODELLER, could only be obtained for this region; however, the secondary structural content of the protein was determined to be 76% helical.[64] Likewise, a reliable structural model for calmodulin-binding domain of the 427 amino acid residue protein channel KCNN4 was retrieved from ModBase (region: 304–377). Since, the template protein–protein complex represents the interaction between calcium-binding domain and calmodulin-binding domain, we pursued the analysis on calcium-binding domain or EF-hand domain of the parasite protein and calmodulin-binding domain of host RBC protein channel KCNN4. The binding pose as observed in the template complex could not be directly extrapolated onto the host–parasite protein pairs, owing to the absence of conservation of interface residues. Thus, we probed the probable binding pose of the host–parasite complex with the help of protein–protein docking program ClusPro2.0.[65] ClusPro2.0 identifies a large number of docked conformations, rigorously evaluates energies of each of the docked protein pairs, and recognizes modeled complexes with near-native conformations, which are usually present in the top-ranking clusters.[66] The putative low-energy docked conformation of the host–parasite protein pair, thus obtained, was probed in terms of surface complementarity and interaction energy of the complex. The calculations on geometrical packing at the interface of the predicted RBC–parasite complex yielded an S_c measure of 0.63, which is highly similar to the S_c score of the template complex of 0.68. The calculations on free energy of binding, pursued using FoldX, yielded an interaction energy value of –18.7 kcal/mol for the template complex, and a relatively better interaction energy value of –30.1 kcal/mol for the modeled complex. In order to support this finding, we investigated further in terms of electrostatic complementarity and interfacial residues stabilizing the modeled complex. The template complex exhibits the predominance of hydrophobic interactions at the interface apart from the long-range electrostatic contacts between positive surface of calmodulin-binding domain and acidic surface of calmodulin, which anchors calmodulin onto calmodulin-binding domain.[63] A similar

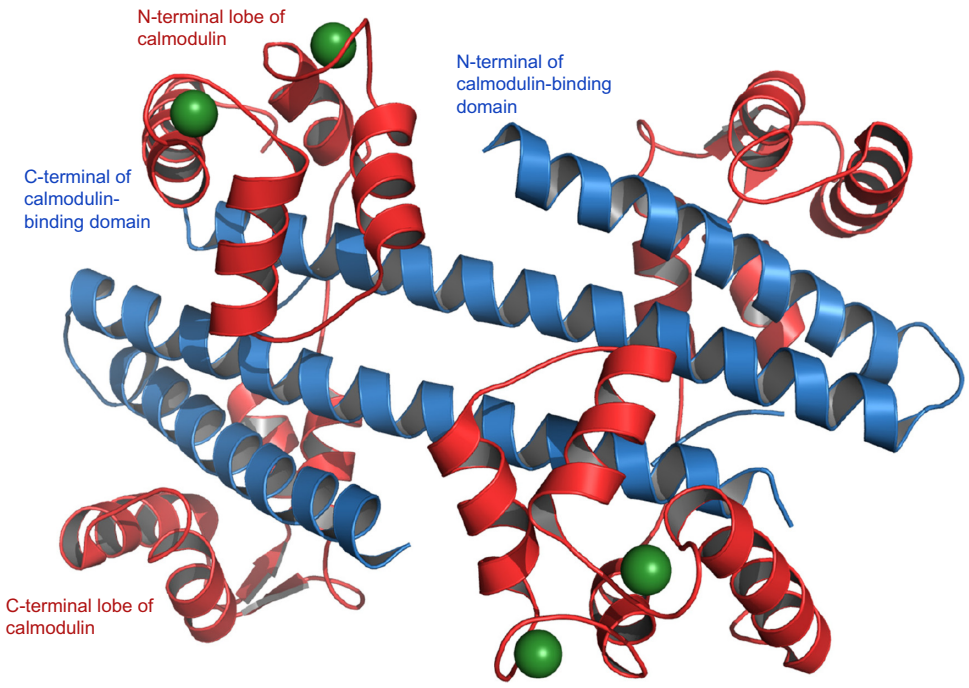

Figure 5. Crystal structures of calmodulin and calmodulin-binding domain are shown in ribbon representation (PDB code: 1G4Y). The blue ribbon represents calmodulin-binding domain, and the red ribbon represents calmodulin with calcium ions depicted as green spheres.

overall electrostatic complementarity could be recognized in the predicted host–parasite complex, demonstrated by positive surface of calmodulin-binding domain of KCNN4 and acidic surface of calcium-binding region of PF3D7_1463900. This observed feature is illustrated in Figure 6, where the interacting host and parasite proteins are rendered as molecular surfaces colored on the basis of their electrostatic potential. The electrostatic properties for the predicted interacting proteins were calculated using Adaptive Poisson-Boltzmann Solver[67] tool availed through Chimera,[68] an extensive resource for molecular visualization and analysis. Figure 7 exemplifies the low-energy binding pose achieved and the probable hydrophobic interactions and electrostatic contacts brought about by residues at the interface contributing to the stabilization of the host–parasite modeled complex. As illustrated in the figure, the hydrophobic interactions are brought about by the residues Leu980 and Ile999 of the parasite protein and Leu319, Val365, and Val369 of the host protein, while the salt bridge forming residues correspond to Asp985, Glu995, and Glu1018 of the parasite protein and Lys312 and Arg362 of the host protein. These details show that similar pattern of interactions is brought about by residues, which are distinct from those

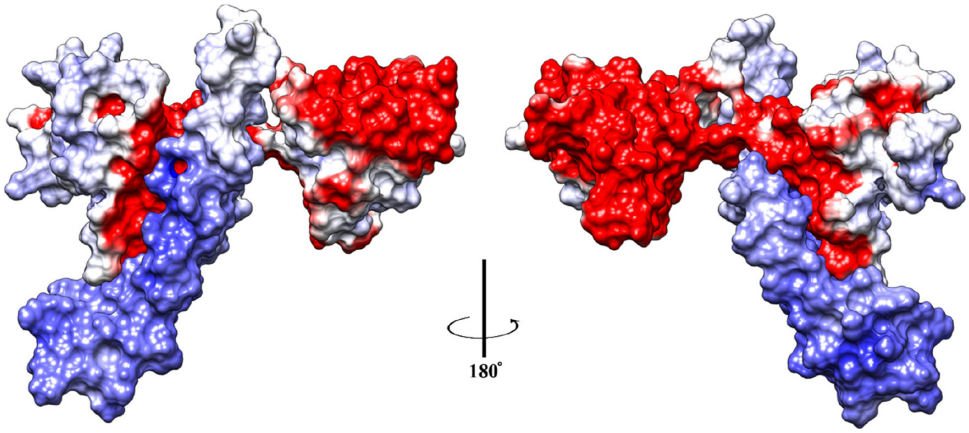

Figure 6. Perspective view of electrostatic complementarity of the modeled host–parasite complex. The host RBC and parasite proteins are rendered as molecular surfaces and are colored based on electrostatic potential (blue: positive, white/gray: neutral, and red: negative). The binding pose of the predicted interaction is illustrated, where the host calmodulin-binding domain in blue is anchored to the C-terminal lobe of EF-hand domain of parasite protein. The two panels show 180° perspective view of the electrostatic contacts between positive and acidic surfaces of host and parasite domains, respectively. This figure is generated using UCSF Chimera[65] (http://www.cgl.ucsf.edu/chimera).

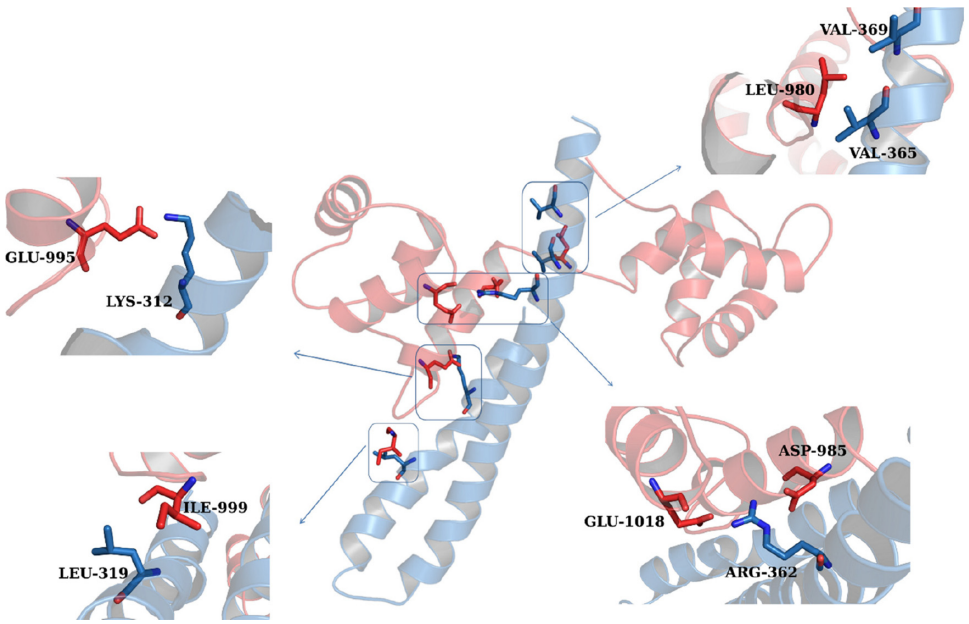

Figure 7. Assessing host–parasite interacting surfaces. The binding pose of host calmodulin-binding domain and parasite EF-hand domain is delineated, where the domains are rendered as transparent ribbons and the putative interacting residues as sticks. Each of the salt bridge forming residues and the residues mediating hydrophobic interactions are highlighted separately. The side chains of the residues highlight hydrogen-bond interactions and hydrophobic interactions.

observed in the template complex.[63] The proposed binding pose for the modeled complex, where the calmodulin-binding domain of KCNN4 interacts predominantly with C-terminal lobe of the EF-hand domain of the parasite, is thus distinct from the pose observed in heterotetrameric template complex (Fig. 5). Such a binding mode could be suggestive of modulation or inhibition of channel activity of host RBCs. The inactivity of calcium-activated potassium channels in parasitized RBCs has been well established previously.[69] The basis of inhibition of host RBC potassium ion channels by the parasite can be theorized owing to the unlikeliness of 1071 residue parasitic protein to dimerize with the calmodulin-binding domain of ion channel. Instead of facilitating gating mechanism of the potassium ion channel, it is plausible that the parasite protein disables the proper functioning of the ion channel, thus, mediating host-cell rupture. The assessment measures, including interaction energy value of –30.1 kcal/mol and electrostatic complementarity of the modeled complex coupled with the evidences on subcellular localization[70] and abundant protein expression during schizont and merozoite growth stages of the parasite,[24] justify the credibility of the predicted host–parasite interaction.

Conclusion

Understanding the intricacies in the strategies acquired by a pathogen to remodel its host-cell machinery for successful colonization and persistence within the host requires understanding of protein–protein interactions across the host and the pathogen. In addition, the construction of protein interaction network for the pathogen can aid in the comprehension of local and global functional relationships within the pathogen, as described earlier,[21] for the multihost parasite *P. falciparum*.

We have demonstrated the usefulness of structure-based approach integrated with various filters in recognizing 208 physicochemically viable protein–protein interactions across 30 host RBC proteins and 59 *P. falciparum* proteins. Integration of additional information pertaining to subcellular localization and protein expression profiles becomes a prerequisite to identify feasible RBC–parasite interactions, owing to the growth and development of the parasite in mature RBCs. The parasite proteins localized solely in cellular compartments, such as apicoplast, may not exhibit physical interaction with the host RBC proteins. Information on subcellular localization and protein expression is crucial especially for parasites such as *P. falciparum*, which reside in heterogeneous environmental conditions at different stages of their life cycle. This step aided in the extraction of RBC–parasite interactions in biological context and elimination of large number of interactions that are unlikely to occur *in vivo*. Indeed, the coverage on potential RBC–parasite interactions identified is limited by the availability of crystal structures of protein complexes. However, despite the limitations, our predictions provide an enriched list of potential players in *P. falciparum* that are capable of remodeling erythrocytes during infection. Analyses on biological pathways and processes potentially influenced due to RBC–parasite interactions suggested a significant role played by parasitic proteins in cytoadherence of infected RBCs and immune evasion. Furthermore, the participation of conserved parasite proteins of unknown function in RBC–parasite interaction necessitates the recognition of structure and function for such proteins. We have also demonstrated rigorous means to analyze and evaluate the functional viability of a predicted interaction in terms of geometrical packing at the interfacial region, electrostatic complementarity of the interacting surfaces, and interaction energies. The RBC–parasite protein–protein interactions, thus predicted, have the potential to warrant experimental endeavors in understanding probable mechanisms of pathogenesis.

Author Contributions

Conceived and designed the experiments: NS, PP, VN. Analyzed the data and contributed to the writing of manuscript: GR. Agreed with manuscript results and conclusions: NS, PP, VN, GR. Made critical revisions and approved the final version: NS. All authors reviewed and approved the final manuscript.

Supplementary Material

Supplementary Table 1. Details on probable interacting proteins across *P. falciparum* and host erythrocyte.

REFERENCES

1. World Health Organization. 2014. *World Malaria Report*. Geneva, Switzerland: World Health Organization.
2. Mackinnon MJ, Marsh K. The selection landscape of malaria parasites. *Science*. 2010;328(5980):866–71.
3. Bannister LH, Hopkins JM, Fowler RE, et al. A brief illustrated guide to the ultrastructure of *Plasmodium falciparum* asexual blood stages. *Parasitol Today*. 2000;16(10):427–33.
4. Maier AG, Cooke BM, Cowman AF, et al. Malaria parasite proteins that remodel the host erythrocyte. Nature reviews. *Microbiology*. 2009;7(5):341–54.
5. Mbengue A, Yam XY, Braun-Breton C. Human erythrocyte remodelling during *Plasmodium falciparum* malaria parasite growth and egress. *Br J Haematol*. 2012;157(2):171–9.
6. Olszewski KL, Morrisey JM, Wilinski D, et al. Host-parasite interactions revealed by *Plasmodium falciparum* metabolomics. *Cell Host Microbe*. 2009;5(2):191–9.
7. Saraogi V, Padmapriya P, Paul A, et al. Change in spectrum of Brownian fluctuations of optically trapped red blood cells due to malarial infection. *J Biomed Opt*. 2010;15(3):037003.
8. Regev-Rudzki N, Wilson DW, Carvalho TG, et al. Cell-cell communication between malaria-infected red blood cells via exosome-like vesicles. *Cell*. 2013;153(5):1120–33.
9. Kotelnikova E, Kalinin A, Yuryev A, et al. Prediction of protein-protein interactions on the basis of evolutionary conservation of protein functions. *Evol Bioinform Online*. 2007;3:197–206.
10. Shen J, Zhang J, Luo X, et al. Predicting protein-protein interactions based only on sequences information. *Proc Natl Acad Sci U S A*. 2007;104(11):4337–41.
11. Aloy P, Russell RB. Interrogating protein interaction networks through structural biology. *Proc Natl Acad Sci U S A*. 2002;99(9):5896–901.
12. Tuncbag N, Gursoy A, Nussinov R, et al. Predicting protein-protein interactions on a proteome scale by matching evolutionary and structural similarities at interfaces using PRISM. *Nat Protoc*. 2011;6(9):1341–54.
13. Zhang QC, Petrey D, Deng L, et al. Structure-based prediction of protein-protein interactions on a genome-wide scale. *Nature*. 2012;490(7421):556–60.
14. Zhou H, Jin J, Wong L. Progress in computational studies of host-pathogen interactions. *J Bioinform Comput Biol*. 2013;11(2):1230001.
15. Davis FP, Barkan DT, Eswar N, et al. Host pathogen protein interactions predicted by comparative modeling. *Protein Sci*. 2007;16(12):2585–96.

16. Krishnadev O, Srinivasan N. A data integration approach to predict host-pathogen protein-protein interactions: application to recognize protein interactions between human and a malarial parasite. *In Silico Biol*. 2008;8(3–4):235–50.
17. Tyagi N, Krishnadev O, Srinivasan N. Prediction of protein-protein interactions between *Helicobacter pylori* and a human host. *Mol Biosyst*. 2009;5(12):1630–5.
18. Krishnadev O, Srinivasan N. Prediction of protein-protein interactions between human host and a pathogen and its application to three pathogenic bacteria. *Int J Biol Macromol*. 2011;48(4):613–9.
19. Ramakrishnan G, Chandra NR, Srinivasan N. From workstations to workbenches: towards predicting physicochemically viable protein-protein interactions across a host and a pathogen. *IUBMB Life*. 2014;66(11):759–74.
20. Gardner MJ, Hall N, Fung E, et al. Genome sequence of the human malaria parasite *Plasmodium falciparum*. *Nature*. 2002;419(6906):498–511.
21. Ramaprasad A, Pain A, Ravasi T. Defining the protein interaction network of human malaria parasite *Plasmodium falciparum*. *Genomics*. 2012;99(2):69–75.
22. Dyer MD, Murali TM, Sobral BW. Computational prediction of host-pathogen protein-protein interactions. *Bioinformatics*. 2007;23(13):i159–66.
23. Wuchty S. Computational prediction of host-parasite protein interactions between *P. falciparum* and *H. sapiens*. *PLoS One*. 2011;6(11):e26960.
24. Aurrecoechea C, Brestelli J, Brunk BP, et al. PlasmoDB: a functional genomic database for malaria parasites. *Nucleic Acids Res*. 2009;37(Database issue):D539–43.
25. D'Alessandro A, Righetti PG, Zolla L. The red blood cell proteome and interactome: an update. *J Proteome Res*. 2010;9(1):144–63.
26. Apweiler R, Bateman A, Martin MJ, et al. Activities at the universal protein resource (UniProt). *Nucleic Acids Res*. 2014;42(D1):D191–8.
27. Mintseris J, Weng Z. Atomic contact vectors in protein-protein recognition. *Proteins*. 2003;53(3):629–39.
28. Choi YS, Yang JS, Choi Y, et al. Evolutionary conservation in multiple faces of protein interaction. *Proteins*. 2009;77(1):14–25.
29. Hwang H, Vreven T, Janin J, et al. Protein-protein docking benchmark version 4.0. *Proteins*. 2010;78(15):3111–4.
30. Finn RD, Miller BL, Clements J, et al. iPfam: a database of protein family and domain interactions found in the protein data bank. *Nucleic Acids Res*. 2014;42(Database issue):D364–73.
31. Berman HM, Westbrook J, Feng Z, et al. The protein data bank. *Nucleic Acids Res*. 2000;28(1):235–42.
32. Finn RD, Bateman A, Clements J, et al. Pfam: the protein families database. *Nucleic Acids Res*. 2014;42(Database issue):D222–30.
33. Fox NK, Brenner SE, Chandonia JM. SCOPe: structural classification of proteins–extended, integrating SCOP and ASTRAL data and classification of new structures. *Nucleic Acids Res*. 2014;42(Database issue):D304–9.
34. Eddy SR. Accelerated profile HMM searches. *PLoS Comput Biol*. 2011;7(10):e1002195.
35. Gough J, Karplus K, Hughey R, et al. Assignment of homology to genome sequences using a library of hidden Markov models that represent all proteins of known structure. *J Mol Biol*. 2001;313(4):903–19.
36. Punta M, Coggill PC, Eberhardt RY, et al. The Pfam protein families database. *Nucleic Acids Res*. 2012;40(Database issue):D290–301.
37. Mohanty S, Srinivasan N. How effective is the data on co-occurrence of domains in multi-domain proteins in prediction of protein-protein interactions? Paper presented at: Genomic Signal Processing and Statistics, 2009. GENSIPS 2009. IEEE International Workshop, Minneapolis, MN, USA; May 17–21, 2009.
38. Florens L, Washburn MP, Raine JD, et al. A proteomic view of the *Plasmodium falciparum* life cycle. *Nature*. 2002;419(6906):520–6.
39. Le Roch KG, Zhou Y, Blair PL, et al. Discovery of gene function by expression profiling of the malaria parasite life cycle. *Science*. 2003;301(5639):1503–8.
40. Pease BN, Huttlin EL, Jedrychowski MP, et al. Global analysis of protein expression and phosphorylation of three stages of *Plasmodium falciparum* intraerythrocytic development. *J Proteome Res*. 2013;12(9):4028–45.
41. Hiller NL, Bhattacharjee S, van Ooij C, et al. A host-targeting signal in virulence proteins reveals a secretome in malarial infection. *Science*. 2004;306(5703):1934–7.
42. Marti M, Good RT, Rug M, et al. Targeting malaria virulence and remodeling proteins to the host erythrocyte. *Science*. 2004;306(5703):1930–3.
43. Heiber A, Kruse F, Pick C, et al. Identification of new PNEPs indicates a substantial non-PEXEL exportome and underpins common features in *Plasmodium falciparum* protein export. *PLoS Pathog*. 2013;9(8):e1003546.
44. Nyalwidhe J, Lingelbach K. Proteases and chaperones are the most abundant proteins in the parasitophorous vacuole of *Plasmodium falciparum*-infected erythrocytes. *Proteomics*. 2006;6(5):1563–73.
45. Lanzer M, Wickert H, Krohne G, et al. Maurer's clefts: a novel multi-functional organelle in the cytoplasm of *Plasmodium falciparum*-infected erythrocytes. *Int J Parasitol*. 2006;36(1):23–36.
46. Cowman AF, Berry D, Baum J. The cellular and molecular basis for malaria parasite invasion of the human red blood cell. *J Cell Biol*. 2012;198(6):961–71.
47. Ginsburg H. Progress in in silico functional genomics: the malaria metabolic pathways database. *Trends Parasitol*. 2006;22(6):238–40.
48. Kraemer SM, Smith JD. A family affair: var genes, PfEMP1 binding, and malaria disease. *Curr Opin Microbiol*. 2006;9(4):374–80.
49. Cruz LN, Wu Y, Craig AG, et al. Signal transduction in plasmodium-red blood cells interactions and in cytoadherence. *An Acad Bras Cienc*. 2012;84(2):555–72.
50. Banumathy G, Singh V, Tatu U. Host chaperones are recruited in membrane-bound complexes by *Plasmodium falciparum*. *J Biol Chem*. 2002;277(6):3902–12.
51. Gilberger TW, Thompson JK, Triglia T, et al. A novel erythrocyte binding antigen-175 paralogue from *Plasmodium falciparum* defines a new trypsin-resistant receptor on human erythrocytes. *J Biol Chem*. 2003;278(16):14480–6.
52. Shiba T, Kawasaki M, Takatsu H, et al. Molecular mechanism of membrane recruitment of GGA by ARF in lysosomal protein transport. *Nat Struct Biol*. 2003;10(5):386–93.
53. Sali A, Blundell TL. Comparative protein modelling by satisfaction of spatial restraints. *J Mol Biol*. 1993;234(3):779–815.
54. Pieper U, Webb BM, Dong GQ, et al. ModBase, a database of annotated comparative protein structure models and associated resources. *Nucleic Acids Res*. 2014;42(Database issue):D336–46.
55. Zhang Y, Skolnick J. TM-align: a protein structure alignment algorithm based on the TM-score. *Nucleic Acids Res*. 2005;33(7):2302–9.
56. Xu J, Zhang Y. How significant is a protein structure similarity with TM-score = 0.5? *Bioinformatics*. 2010;26(7):889–95.
57. Pronk S, Pall S, Schulz R, et al. GROMACS 4.5: a high-throughput and highly parallel open source molecular simulation toolkit. *Bioinformatics*. 2013;29(7):845–54.
58. Lawrence MC, Colman PM. Shape complementarity at protein-protein interfaces. *J Mol Biol*. 1993;234(4):946–50.
59. Schymkowitz J, Borg J, Stricher F, et al. The FoldX web server: an online force field. *Nucleic Acids Res*. 2005;33(Web Server issue):W382–8.
60. Albano FR, Berman A, La Greca N, et al. A homologue of Sar1p localises to a novel trafficking pathway in malaria-infected erythrocytes. *Eur J Cell Biol*. 1999;78(7):453–62.
61. Taraschi TF, Trelka D, Martinez S, et al. Vesicle-mediated trafficking of parasite proteins to the host cell cytosol and erythrocyte surface membrane in *Plasmodium falciparum* infected erythrocytes. *Int J Parasitol*. 2001;31(12):1381–91.
62. Pietrobon D, Di Virgilio F, Pozzan T. Structural and functional aspects of calcium homeostasis in eukaryotic cells. *Eur J Biochem*. 1990;193(3):599–622.
63. Schumacher MA, Rivard AF, Bachinger HP, et al. Structure of the gating domain of a Ca2+-activated K+ channel complexed with Ca2+/calmodulin. *Nature*. 2001;410(6832):1120–4.
64. Buchan DW, Minneci F, Nugent TC, et al. Scalable web services for the PSIPRED protein analysis workbench. *Nucleic Acids Res*. 2013;41(Web Server issue):W349–57.
65. Comeau SR, Gatchell DW, Vajda S, et al. ClusPro: a fully automated algorithm for protein-protein docking. *Nucleic Acids Res*. 2004;32(Web Server issue):W96–9.
66. Comeau SR, Gatchell DW, Vajda S, et al. ClusPro: an automated docking and discrimination method for the prediction of protein complexes. *Bioinformatics*. 2004;20(1):45–50.
67. Baker NA, Sept D, Joseph S, et al. Electrostatics of nanosystems: application to microtubules and the ribosome. *Proc Natl Acad Sci U S A*. 2001;98(18):10037–41.
68. Pettersen EF, Goddard TD, Huang CC, et al. UCSF Chimera–a visualization system for exploratory research and analysis. *J Comput Chem*. 2004;25(13):1605–12.
69. Staines HM, Chang W, Ellory JC, et al. Passive Ca(2+) transport and Ca(2+)-dependent K(+) transport in *Plasmodium falciparum*-infected red cells. *J Membr Biol*. 1999;172(1):13–24.
70. van Ooij C, Tamez P, Bhattacharjee S, et al. The malaria secretome: from algorithms to essential function in blood stage infection. *PLoS Pathog*. 2008;4(6):e1000084.
71. *The PyMOL Molecular Graphics System, Version 1.4.1*. Schrodinger, L.L.C. http://www.pymol.org